

Synthesis of a Thin-Layered Ionic Conductor, CeO₂–Y₂O₃, by Atomic Layer Deposition in View of Solid Oxide Fuel Cell Applications

Elise Ballée,[†] Armelle Ringuedé,[†] Michel Cassir,^{*,†} Matti Putkonen,^{‡,§} and Lauri Niinistö[‡]

[†]Laboratoire d'Electrochimie, Chimie des Interfaces et Modélisation pour l'Energie, UMR 7575 CNRS, Chimie ParisTech, 11 rue Pierre et Marie Curie, F-75231 Paris Cedex 05, France, and [‡]Laboratory of Inorganic and Analytical Chemistry, Helsinki University of Technology (TKK), FI-02015 Espoo, Finland.
[§] Present address: Beneq Ltd, Ensimmäinen savu, FI-01510 Vantaa, Finland

Received June 18, 2009. Revised Manuscript Received July 28, 2009

Thin films of yttria-doped ceria (YDC) electrolyte were processed for the first time by atomic layer deposition (ALD) for solid oxide fuel cell (SOFC) applications. The β -diketonate complexes Y(thd)₃ and Ce(thd)₄ were used as yttrium and cerium precursors, respectively, whereas ozone was used as the oxygen source. Four-hundred-nanometer thick YDC films were deposited at 300 °C on soda lime, Si(100), stainless steel (430), La_{0.8}Sr_{0.2}FeO₃ (LSF) cathodes, and on Ni-YSZ anodes. Thickness, crystallinity, and morphology of YDC films were determined by UV–vis spectroscopy, XRD, and SEM/EDX, respectively. Electrical properties of the thin films in the range of 250–475 °C were characterized by impedance spectroscopy. The deposited layers were crystalline as deposited, without any need for annealing. SEM observations showed that the films were homogeneous and well-covering. Their conductivities were significantly lower than those reported in the literature for bulk YDC. Nevertheless, electrical properties of YDC thin films seem to be superior to those of the YSZ thin films, characterized under the same conditions, in the temperature range of 500–750 °C. Thus, YDC by ALD represents a new and promising SOFC generation.

Introduction

The industrial development and use of SOFC devices is presently limited by their working temperature which ranges from 800 to 1000 °C. Most of the research is therefore oriented toward decreasing their operational temperature to 600–700 °C, which would allow the use of cheaper interconnects and current collectors, as well as to control thermal constraints, which could otherwise result in a rapid aging of the cell materials. Moreover, the fabrication and operation costs should also be reduced.

To reach these goals, the most promising route involves the use of electrolytes, at least as conductive as yttria-stabilized zirconia (YSZ), in the form of thin layers (< 5 μ m), as recently reported in several papers.^{1–7} In the temperature range envisaged, the ionic conductivity

of ceria-based electrolytes (Ce_{1-x}M_xO_{2- δ} , where M is the doping cation) is equal or superior to that of zirconia-based electrolytes, as shown in Figure 1, which is based on literature data.⁸ As in the case of zirconia, it is observed also for the ceria materials that the closer the ionic radius of the dopant is with respect to that of cerium ion, the higher is the conductivity. The relevant values of ionic radii in nm with CN = 6 (this available configuration was taken, as a first approximation, instead of CN = 8 in the real environment of the material) are: Ce⁴⁺ (0.092), Y³⁺ (0.090), Gd³⁺ (0.094), Sm³⁺ (0.096);⁹ therefore, most of the studies have been focused on gadolinia-doped ceria (GDC). The deposits synthesized by atomic layer deposition, ALD, have a high microstructural quality, i.e., YSZ ultrathin deposits are dense, well-covering, uniform, adherent, and crystalline without need for an annealing post-treatment.^{6,7,10–14} Nevertheless, the composition of

*Corresponding author. Phone: 00-33-1-55426387. Fax: 00-33-1-44276750. E-mail: michel-cassir@enscp.fr.

- (1) Beckel, D.; Bieberle-Hütter, A.; Harvey, A.; Infortuna, A.; Muecke, U. P.; Prestat, M.; Rupp, J. L. M.; Gauckler, L. J. *J. Power Sources* **2007**, *173*, 325–345.
- (2) Kosacki, I.; Susuki, T.; Anderson, H. U.; Colomban, P. *Solid State Ionics* **2002**, *149*, 99–105.
- (3) Jud, E.; Huwiler, C. B.; Gauckler, L. J. *J. Am. Ceram. Soc.* **2005**, *88*, 3013–3019.
- (4) Musil, J.; Baroch, P.; Vleck, J.; Nam, K. H.; Han, J. G. *Thin Solid Films* **2005**, *475*, 208–218.
- (5) Fahlman, B. D. *Curr. Org. Chem.* **2006**, *10*, 1021–1033.
- (6) Bernay, C.; Ringuedé, A.; Colomban, P.; Lincot, D.; Cassir, M. J. *Phys. Chem. Solids* **2003**, *64*, 1761–1770.
- (7) Brahim, C.; Ringuedé, A.; Cassir, M.; Putkonen, M.; Niinistö, L. *Appl. Surf. Sci.* **2007**, *253*, 3962–3968.

- (8) Kharton, V. V.; Marques, F. M. B.; Atkinson, A. *Solid State Ionics* **2004**, *174*, 135–149.
- (9) Shannon, R. D. *Acta Crystallogr., Sect. A* **1976**, *32*, 751–767.
- (10) Brahim, C. Ph.D. Thesis, ENSCP, University of Paris 6, Paris, **2006**.
- (11) Brahim, C.; Ringuedé, A.; Cassir, M.; Putkonen, M.; Niinistö, L. *ECS Trans.* **2007**, *15*, 261–268.
- (12) Eisentraut, K. J.; Sievers, R. E. *J. Am. Chem. Soc.* **1965**, *87*, 5254–5259.
- (13) Putkonen, M.; Sajavaara, T.; Niinistö, J.; Johansson, L. S.; Niinistö, L. *J. Mater. Chem.* **2002**, *12*, 442–448.
- (14) Shim, J. H.; Chao, C.-C.; Huang, H.; Prinz, F. B. *Chem. Mater.* **2007**, *19*, 3850–3854.

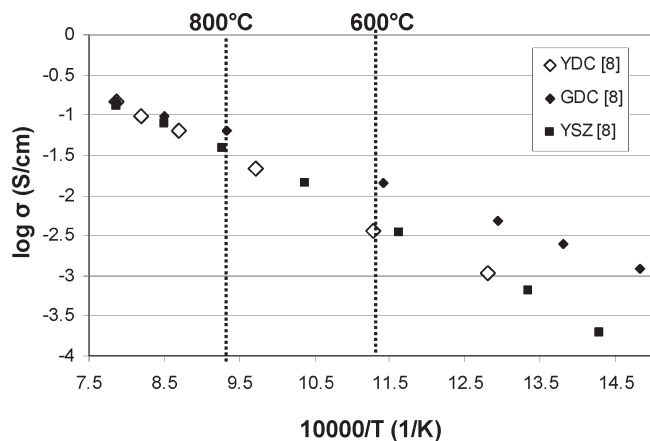


Figure 1. Conductivity of zirconia- or ceria-based compounds: YSZ, YDC, and GDC (gadolinia-doped ceria) pellets in air.⁸

GDC films deposited by ALD has proven to be difficult to optimize and the growth rate is generally very low, i.e., 0.4–0.5 Å/cycle.^{15,16} Yttria could be a good substitute for gadolinia, as the Y^{3+} ionic radius is similar to that of Gd^{3+} and ALD processes for Y_2O_3 deposits are well-established with more satisfactory growth rates.¹³ Furthermore, the use of yttria-doped ceria (YDC) could introduce a lower cost solution for an ALD-based SOFC electrolyte, due to the fact that yttrium is more abundant than gadolinium.¹⁷

ALD is an advanced chemical method to grow thin films and thin film structures. It is especially well-suited for the deposition of oxide films.¹⁸ ALD has also recently evolved as a method of choice for nanotechnology.¹⁹ The precursors used in the ALD technology for oxides should be volatile, stable in the gas phase, but at the same time possess sufficient reactivity toward the oxygen source, which is usually water, oxygen, or ozone. The β -diketonates meet these requirements and have therefore been extensively applied in ALD,²⁰ although other precursors are also available.²¹ ALD processes for yttrium and cerium oxides have been based on β -diketonates and ozone, reacting at substrate temperatures higher than 400 °C.^{22,23} These processes and precursors were later

refined to allow depositions at significantly lower temperatures.^{24,25} Also, the radical-enhanced ALD of Y_2O_3 from β -diketonate precursor and oxygen radicals results in lower deposition temperatures.²⁶

The aim of this work was to analyze for the first time the feasibility of yttria-doped ceria (YDC) synthesis by ALD on different substrates, including SOFC electrodes, to be followed by a thorough study on the structural, morphological, and electrical properties of the materials obtained.

Experimental Section

Thin Film Deposition. Yttria-doped ceria thin films were deposited in a commercial flow-type hot-wall ALD reactor F-120 manufactured by ASM Microchemistry Ltd. (Helsinki, Finland). Film depositions were carried out at 1–3 mBar pressure. $Y(thd)_3$ and $Ce(thd)_4$ ($thd = 2,2,6,6$ -tetramethylheptane-3,5-dionate) were synthesized by procedures described earlier.^{24,25} Ozone was employed for oxidation and was produced from oxygen (> 99.999%) in an ozone generator (Fischer, del 502).

Yttrium and cerium precursors and ozone were transported onto the substrate with nitrogen carrier gas (> 99.999%, Schmidlin UHPN 3000 N_2 generator). The purge time for nitrogen was 2 s. The experimental precursor pulsing times were kept long enough in order to achieve surface saturation on the planar substrate.

Soda lime glass ($5 \times 5 \text{ cm}^2$), silicon(100) wafers (from Okmetic, Vantaa, Finland; cut to $5 \times 5 \text{ cm}^2$), stainless steel (Goodfellow 430, Fe81/Cr17/Mn/Si/C/S/P, 0.7 mm thick, annealed, $1 \times 1 \text{ cm}^2$), LSF, $La_{0.8}Sr_{0.2}FeO_3$ (Praxair powder pressed and annealed at 1000 °C during 2 h, $1 \times 1 \text{ cm}^2$), and Ni-YSZ (INDEC anode, $1 \times 1 \text{ cm}^2$) were used as substrates. Substrates were ultrasonically cleaned in acetone and ethanol before use.

Characterization Methods. Thickness, structure, and morphology of YDC films, as well as their electrical properties, were determined ex situ. Crystallinity was determined by X-ray diffraction (XRD) using $Co K\alpha$ radiation (1.7890 Å) in a Siemens D5000 diffractometer with 2θ varying from 15 to 75°. The diffraction pattern was scanned in steps of 0.02° with 2 s counting times. The grain size was evaluated using the Scherrer formula²⁷

$$d = \frac{0.9\lambda}{b \cos \theta}$$

where 0.9 is the Scherrer shape factor, λ the X-ray wavelength, b the full width at half-maximum (fwhm) of the sample peak, and θ the diffraction angle of the peak considered.

Thickness was determined by a spectrophotometric method.²⁸ Reflectance spectra were recorded in the wavelength region 190–1100 nm for Si(100) substrates. The spectra were fitted to obtain geometric thickness. Measurements were performed in a Hitachi U-2000 spectrophotometer. Microstructure was evaluated from cross-sectional scanning electron microscopy (SEM) micrographs obtained in S440 Leica SEM.

The yttrium to cerium ratio was measured by X-ray fluorescence, XRF (Philips PW 1480 WDS spectrometer) using Rh excitation. Data were analyzed with the UNIQANT 4.34 program.²⁹

- (15) Gourba, E.; Ringuédé, A.; Cassir, M.; Päiväsaari, J.; Niinistö, L.; Putkonen, M.; Niinistö, L. *Proceedings of the 8th International Symposium on Solid Oxide Fuel Cells*; Paris, April 27–May 2, 2003; Singhal, S.C., Dokiya, M., Eds.; The Electrochemical Society: Pennington, NJ, 2003; Vol. 7, pp 267–274.
- (16) Gourba, E.; Ph.D. Thesis, ENSCP, University of Paris 6, France, 2004.
- (17) Taylor, S. R. *Geochim. Cosmochim. Acta* **1964**, *28*, 1280–1284.
- (18) Niinistö, L.; Päiväsaari, J.; Niinistö, J.; Putkonen, M.; Nieminen, M. *Phys. Status Solidi A* **2004**, *201*, 1443–1452.
- (19) Knez, M.; Nielsch, K.; Niinistö, L. *Adv. Mater.* **2007**, *19*, 3425–3438.
- (20) Tiitta, M.; Niinistö, L. *Chem. Vap. Deposition* **1997**, *3*, 167–182.
- (21) Päiväsaari, J.; Niinistö, J.; Myllymäki, P.; Dezelah, C.; Winter, C. H.; Putkonen, M.; Nieminen, M.; Niinistö, L. *Top. Appl. Phys.* **2007**, *106*, 15–32.
- (22) Mölsä, H.; Niinistö, L.; Utriainen, M. *Adv. Mater. Opt. Electron.* **1994**, *4*, 389–400.
- (23) Mölsä, H.; Niinistö, L.; Utriainen, M. *Mater. Res. Soc. Symp. Proc.* **1994**, *355*, 341–350.
- (24) Putkonen, M.; Sajavaara, T.; Johansson, L.-S.; Niinistö, L. *Chem. Vap. Deposition* **2001**, *7*, 44–50.
- (25) Päiväsaari, J.; Putkonen, M.; Niinistö, L. *J. Mater. Chem.* **2002**, *12*, 1828–1832.

(26) Van, T. T.; Chang, J. P. *Surf. Sci.* **2005**, *596*, 1–11.

(27) Scherrer, P. *Gött. Nachr.* **1918**, *2*, 98–100.

(28) Ylilampi, M.; Ranta-aho, T. *Thin Solid Films* **1993**, *232*, 56–62.

(29) Brahim, C.; Chauveau, F.; Ringuédé, A.; Cassir, M.; Putkonen, M.; Niinistö, L. *J. Mater. Chem.* **2009**, *19*, 760–766.

The electrical properties of the as-deposited films (without any annealing treatment) were analyzed by impedance spectroscopy. These measurements were carried out under ambient air, using an Autolab potentiostat PGSTAT30 with 200 mV ac signal amplitude (ΔV) and without dc polarization in the 1 MHz to 10 mHz frequency range (11 points per decade) in a temperature range varying from 250 to 475 °C. To avoid short-circuits or damage to the deposits no Pt ink was used to contact the electrode. A pointed Pt electrode, constituted by a melted platinum wire with a diameter of 0.5 mm was used as the working electrode. Optical microscopy observations allowed us to evaluate the contact area after measurements, obtaining $S 0.1 \text{ mm}^2$ (diameter is $0.36 \pm 0.02 \text{ mm}$). A Pt spiral was used as the counter-electrode. The experimental setup, allowing to perform the crossover ionic conductivity measurements, was described in a previous paper.²⁹ Impedance diagrams were analyzed using equivalent circuit simulation software (Equivcrt), commercialized by B.A. Boukamp.³⁰

Results and Discussion

YDC Deposition. Surface-controlled deposition of the binary oxides Y_2O_3 and CeO_2 by ALD using $\text{Y}(\text{thd})_3$ and $\text{Ce}(\text{thd})_4$ can be observed in the temperature ranges 250–350 and 175–250 °C, respectively.^{24,25} Nevertheless, the process to grow Y_2O_3 thin films from $\text{Y}(\text{thd})_3$ at temperatures below 300 °C is not entirely optimal,²⁴ whereas the deposition of ceria thin films gives satisfactory results at 300 °C, with a uniform surface-controlled growth.²⁵ It should be noted that with some β -diketonate-based processes the ALD-growth is still maintained although the deposition rate is increased slightly above the nominal “ALD-window”. This is most probably related to partially decomposing ligands or to a change in the adsorption mode yielding higher precursor saturation at surface (molecules/nm²) and thus higher deposition rate. All things considered, the deposition temperature for YDC thin films was chosen as 300 °C. The sublimation temperatures for $\text{Y}(\text{thd})_3$ and $\text{Ce}(\text{thd})_4$ sources, at the prevailing 1–3 mBar pressure, were fixed at 125 and 150 °C, respectively.^{10,22} Even if the literature reports 0.8 and 1 s as pulsing times for yttrium and cerium precursors, respectively,^{24,25} longer pulsing times were applied here in order to saturate the surface at 300 °C. In fact, for each precursor, we have analyzed the growth speed of the film vs the pulsing time on soda-lime glass and found 1.5 s for $\text{Ce}(\text{thd})_4$ to achieve surface saturation. In the case of $\text{Y}(\text{thd})_3$, only 1 s was necessary. Therefore, we imposed 1.5 s for both precursors. The standard pulsing sequence combines a certain number of pulsing sequences of $\text{Ce}(\text{thd})_4$ depending on the required yttrium concentration in the YDC thin film, followed by one pulsing sequence of $\text{Y}(\text{thd})_3$, as shown in Table 1.

The relative amount of Y pulses in the total metal pulses was varied from 10 to 75% in order to reach the desired % Y content in the YDC films (Figure 2). Therefore, even though the relation is not really linear, it is relatively straightforward to deposit a film having the desired Ce:Y ratio. Nevertheless, it should be noted that

Table 1. Pulsing Sequence Is one ALD Growth Cycle of YDC

pulse 1: $\text{Ce}(\text{thd})_4$ for 1.5 s	pulse 5: $\text{Y}(\text{thd})_3$ for 1.5 s
pulse 2: N_2 for 2 s	pulse 6: N_2 for 2 s
pulse 3: O_3 for 1.5 s	pulse 7: O_3 for 1.5 s
pulse 4: N_2 for 2 s	pulse 8: N_2 for 2 s

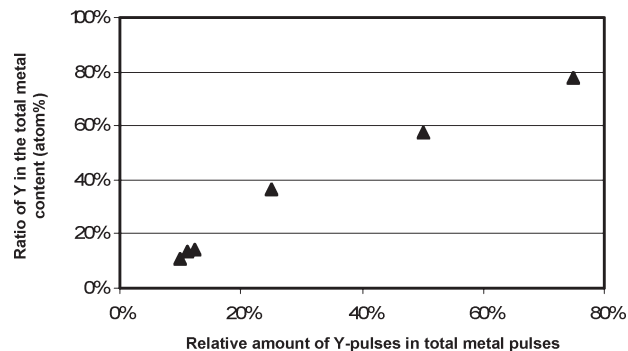


Figure 2. Relative amount of Y in the total metal content of the films as analyzed by XRF.

at an atomic ratio level the deposition of Y occurs at somewhat higher level than Ce, which was already observed by O. Nilsen et al. for calcium-substituted lanthanum ,anganite deposited by ALD.³¹ The composition of the deposited layers was first determined by XRF and then checked by an energy-dispersive X-ray spectrometry (EDX) analysis. XRF analysis remained more accurate and the compositional values obtained by this technique were kept for the rest of the study. An example of composition, thickness, and growth rate measurements in the case of successive deposits by ALD at 300 °C on soda-lime glass is reported in Table 2. Nine YDC samples of roughly 400 nm thickness YDC were obtained with three different compositions, on all the substrates mentioned. Roughly, using pulsing ratios of Ce:Y = 9:1 and 8:1 and 7:1, thin films containing 11.5 at % Y, 13.0 at % Y, and 16 at % Y, respectively, were obtained. It can be observed that the higher the Y content is in YDC, the higher is the growth rate being roughly, from 0.40 Å/cycle for 11.5 at % Y to 0.53 Å/cycle for 16.0 at % Y. These values are higher than that corresponding to the growth rate of Y_2O_3 , 0.23 Å/cycle,²⁴ and approximately similar to that of CeO_2 , 0.42 Å/cycle.²⁵

Structural and Morphological Characterization. *XRD Analysis.* Figure 3 shows XRD patterns of yttria-doped ceria deposited on porous cathode LSF. When compared to the JCPDS card (75–0175), the peaks of our yttria-doped ceria are clearly defined. The sample deposited by ALD (Figure 3b) is well-crystallized without any annealing post-treatment. This is quite remarkable because in this case the ALD process occurs at relatively low temperatures.

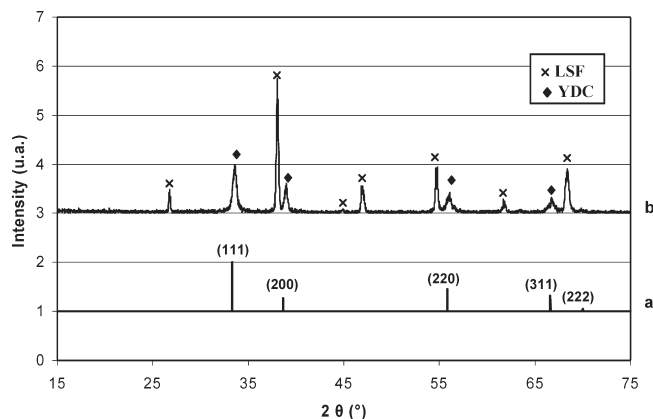
Yttria-doped ceria crystallizes in the cubic structure regardless of the amount of yttrium in the YDC films. This was verified by the three compositions studied. Lattice parameter a was evaluated to 5.4 Å and the average crystallite height was 150 Å. This value was

(30) Boukamp, B. A. *Solid State Ionics* **1986**, *20*, 31–44.

(31) Nilsen, O.; Rauwel, E.; Fjellvåg, H.; Kjekshus, A. *J. Mater. Chem.* **2007**, *17*, 1466–1475.

Table 2. Composition (By XRF), Thickness (By Spectrophotometry), and Growth Rate of YDC Thin Layers Processed By ALD on Soda-Lime Glass Substrates at 300°C

pulsing sequence	composition in at % Y	film thickness (nm)	growth rate (Å/cycle)
Ce7/Y14 successive deposits	14.9	105 ± 5	0.527 ± 0.003
	16.2	106 ± 5	0.530 ± 0.003
	15.7	115 ± 6	0.573 ± 0.003
	16.2	99 ± 5	0.495 ± 0.003
	average: 15.7	total thickness: 425 ± 20	
Ce8/Y14 successive deposits	13.2	96 ± 5	0.425 ± 0.003
	13.2	95 ± 5	0.422 ± 0.003
	13.1	93 ± 5	0.412 ± 0.003
	12.2	96 ± 5	0.428 ± 0.003
	average: 12.9	total thickness: 380 ± 20	
Ce9/Y14 successive deposits	11.9	99 ± 5	0.395 ± 0.002
	11.6	101 ± 5	0.403 ± 0.002
	11.4	101 ± 5	0.403 ± 0.002
	11.2	97 ± 5	0.389 ± 0.002
	average: 11.5	total thickness: 400 ± 20	

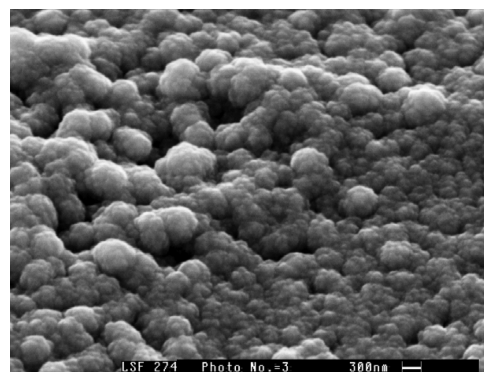
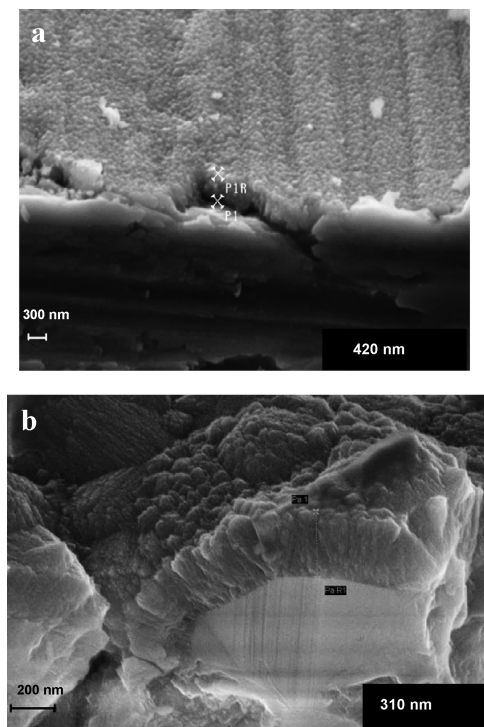
**Figure 3.** XRD patterns of yttria-doped ceria. (a) JCPDS card 75-0175: $Y_{0.20}Ce_{0.80}O_{1.90}$. (b) YDC thin layer deposited by ALD (380 nm thick, 13 at % Y) on LSF.

calculated from the fwhm value of the strongest peak (111) using the Scherrer formula.²⁷ In contrast to the case of a porous LSF cathode, XRD patterns of YDC deposited on silicon or on soda-lime glass were less resolved from the background and difficult to exploit, as only the (311) peak was clearly observable.

SEM Analysis. Morphology of the YDC thin layers deposited was observed by SEM. Films deposited on four different substrates (stainless steel, LSF cathode, Ni-YSZ anode) were analyzed. In all cases, the thin films deposited were, in general, dense, well-covering, and uniform, which are the fundamental requirements for a successful SOFC application.

It appears that the morphology of the substrate has an influence on the growth of thin films (Figures 4 and 5). SEM micrographs clearly showed that YDC grown on stainless steel follows the features existing on the surface, whereas YDC on LSF or NiO/YSZ grew with a distinct “cauliflowers” pattern.

Figure 4 shows some irregularities on the thin layer deposited on the porous SOFC cathode. It is most probably due to the morphology of the substrate more than to a porosity of the layer. Nevertheless, it shows that in the case of an electrolyte processed by ALD, the layer should be thicker to avoid such irregularities that might limit the application.

**Figure 4.** SEM micrograph of yttria-doped ceria layers deposited by ALD at 300 °C on LSF (425 nm thick, 16 at % Y).**Figure 5.** Cross-sectional SEM micrograph of yttria-doped ceria deposited by ALD at 300 °C: (a) on stainless steel (400 nm thick, 11.5 at % Y); (b) Ni-YSZ anode (342 nm thick, 13 at % Y).

Cross-sectional micrographs validated the thickness values obtained by UV spectrophotometry (Figure 5).

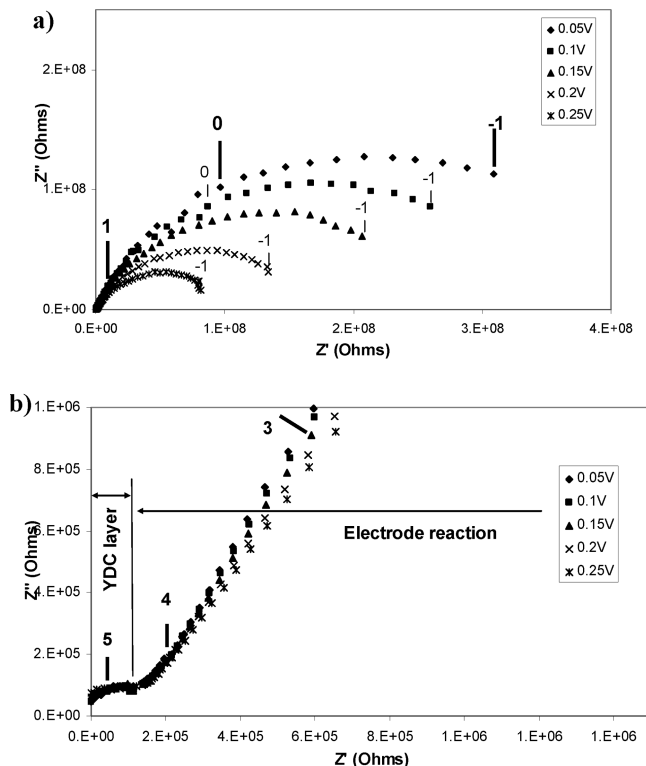


Figure 6. Evolution at 400 °C of the impedance response with the signal amplitude for YDC thin layer deposited by ALD on stainless steel (425 nm thick, 16 at % Y). (a) Nyquist diagrams (frequency logarithms of the applied alternative signal are presented); (b) enlargement of (a).

An average of several measurements gave a 400 nm layer thickness.

Electrical Properties by Impedance Spectroscopy. The evolution with temperature of the electrical characteristics of the impedance response in the YDC electrolyte thin layer, i.e., the resistance, conductivity, activation energy, relaxation frequency, equivalent capacitance, and relative permittivity were analyzed for the YDC electrolyte thin layer. The YDC samples were first submitted to a stability test consisting of measuring the Nyquist impedance diagrams from the highest to the lowest frequencies and reversely. This test showed that the YDC system is stable with a perfect superposition of the forward and backward diagrams.

Figure 6a shows typical Nyquist impedance diagrams obtained at 400 °C for the YDC thin film deposited on stainless steel (16 at % Y, 425 nm thick) at different ac signal amplitudes. The question was to determine the origin of the impedance response. The enlargement of the diagram shows that the first high-frequency semicircle (from 1×10^6 to 1×10^4 Hz) is not affected by the signal amplitude whereas the second low frequency one obviously is (Figure 6b). Thus, it is easy to distinguish the contribution due to the YDC thin layer intrinsic properties from that of the electrode reaction mechanisms. The semicircle obtained at high frequencies allowed us to evaluate the electrolyte resistance and, consequently, the conductivity of YDC and the related activation energy. The second semicircle evolves with the magnitude of the applied potential and is due to the electrode

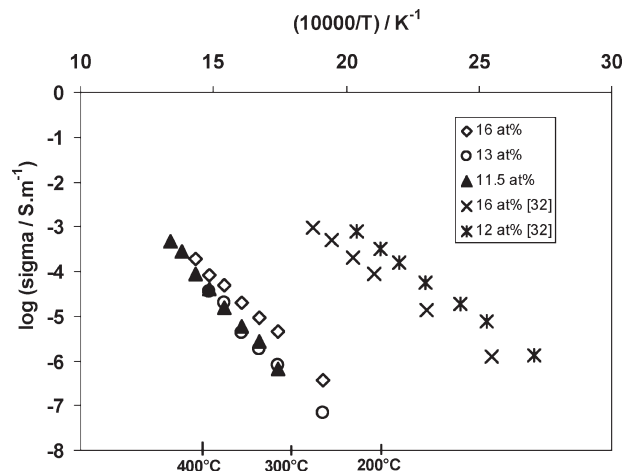


Figure 7. Arrhenius plots of the YDC layer conductivity for samples deposited by ALD as well as those for the YDC bulk.³²

reaction. The conductivity Arrhenius diagrams corresponding to the three analyzed compositions of YDC are plotted in Figure 7. The same figure also depicts the conductivity values obtained on bulk YDC materials. At a given temperature and composition, the total conductivity of the bulk YDC material is superior to that of the YDC thin layer; for instance, in the case of the 16 at % Y at 400 °C, the thin layer is about 350 times less conductive than the bulk sample. A similar situation has been found in other ultrathin layers deposited by ALD, viz. YSZ,^{6,16} IDZ (india-doped zirconia),^{10,11,29} and GDC (gadolinia-doped ceria).^{6,15,16}

It should be kept in mind that in the case of thin layers less than 10 μm thick, according to the results of Gourba,¹⁶ the conductivity is

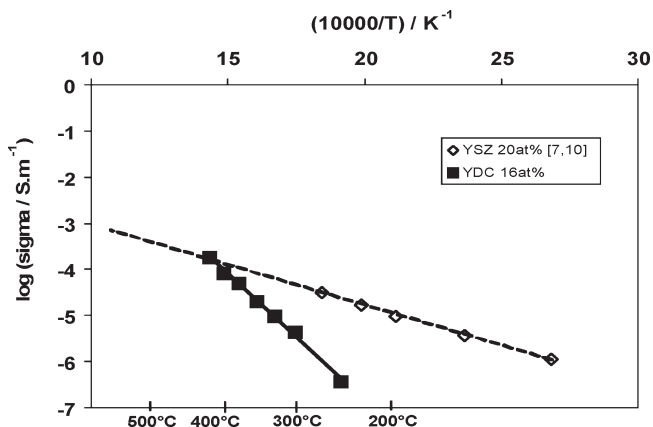
$$\sigma = \frac{l}{RS}$$

with l/S , the geometric factor; l , the thickness of the deposited layer; and S , the surface of the Pt point electrode. Thus, in the case of the thin layers, the main difficulty is to give a good estimation for the surface of the point electrode. Furthermore, as also shown by Gourba,¹⁶ the surface of the point electrode is always overestimated, which partially explains the low conductivities deduced. To get a more precise value of this surface, a modeling effort is required. The microstructure of the layers deposited by ALD could also have an influence on the impedance measurements. In fact, the structure of these layers is constituted by very narrow columns, separated by column boundaries. The conductivity can be seen as the combination of two parallel pathways, one by the columns and the other by the boundaries. This kind of phenomenon requires a deeper insight and precise measurements, which is out of the frame of this paper.

The activation energies were deduced from the Arrhenius diagrams and are reported in Table 3. A decrease in the activation energy can be noted when the content of Y increases from 11.5 to 16 at%. Nevertheless, the activation energy is not significantly different, at a given

Table 3. Activation Energies for YDC Thin Layers Processed by ALD on Stainless Steel at 300 °C; Bulk Value Given by Comparison

E_a (eV)	composition at % Y	thickness (nm)
1.39 ± 0.18	11.5 ± 0.5	400 ± 20
1.27 ± 0.17	13 ± 0.5	380 ± 20
1.09 ± 0.14	16 ± 0.5	425 ± 20
0.92^{31}	16	bulk

**Figure 8.** Arrhenius plots of YDC (16 at % Y) and YSZ (8 at % Y),^{7,10} with a thickness of 425–450 nm, processed by ALD at 300 °C on stainless steel.

composition, i.e. Sixteen at% Y, as compared to the thin layered YDC (1.09 eV) and YDC bulk material (0.92 eV).^{32,33} The results in the literature concerning the influence of thin layers on the activation energy are sometimes contradictory, i.e. in the case of YSZ deposited by ALD, we have found a decrease in the activation energy with respect to bulk YSZ.⁷ Further dedicated studies are surely necessary to be able to understand what are the dominating parameters influencing the activation energy when a bulk material is compared to a thin-layered one.

Afterward, the relaxation frequencies for the thin-layered samples were determined, showing an Arrhenius behavior. The relation $\log f_{\text{relaxation}} = \text{function}(1/T)$ has the same slope for the three analyzed thicknesses and, therefore, the related activation energies are approximately similar, around 0.9–1.0 eV. The equivalent capacitance values, C , were deduced from the relaxation frequencies. Whatever the yttrium content is, the equivalent capacitance stays around 1×10^{-11} F. Finally, the average values of the relative permittivity, ϵ_r , were determined from the average values of the equivalent capacitance, using the classical formula $C = \epsilon_0 \epsilon_r (S/e)$, with $\epsilon_0 = 8.854187 \times 10^{-12}$ F/m, the vacuum permittivity).

The values obtained slightly vary from 1 to 6.5 depending on the yttrium concentration. These values are significantly lower than 55, which is the estimated value reported in the literature for the YDC bulk material.³² If the geometric factor is correctly estimated, it can be

deduced that the YDC thin layer would be a better dielectric material than the bulk YDC material. This then means that when these materials are submitted to increasing electrical fields, YDC processed by ALD would better resist the discharge.

A comparison of the Arrhenius conductivity diagrams of YDC and YSZ¹⁰ is given in Figure 8. At very low temperatures, YSZ is more conductive than YDC, but from 420 °C onward, this tendency is reversed, which explains the current interest of using YDC as an SOFC electrolyte under operating conditions, which are significantly higher than 450 °C.

Conclusions

Very thin layers of YDC were produced for the first time by ALD. The depositions were performed at 300 °C, using Y(thd)₃ and Ce(thd)₃ precursors, on four different substrates: soda-lime glass, stainless steel as well as SOFC cathode and anode materials, respectively, viz. LSF and Ni-YSZ. The process was optimized yielding uniform and dense layers, of about 400 nm thickness which contained Y in the range of 10 to 20 at %. The films are well-covering and adherent regardless the substrate. They are well-crystallized in the cubic structure regardless of the amount of yttrium and needing no annealing treatment; this can be considered as one of the greatest advantages of the ALD deposits. The lattice parameter of YDC is 5.4 Å and the average crystallite size 150 Å.

Arrhenius diagrams showed that the total conductivity of the ALD-processed YDC is significantly lower than that of the bulk material. This difference has already been observed with other ALD-processed films⁷ and it might be due either to an overestimated value of the geometric factor l/S , or to the particular microstructure of the ALD-processed thin films. The use of a nonrigorously adapted conductivity formula is also a possible reason for the low conductivity value measured for the ALD films.

In contrast, the activation energies obtained are approximately similar for both YDC thin layer and bulk material, with an average value of 1.1 ± 0.1 eV for the 16 at % Y sample. The activation energy decreases as the ratio of Y to Ce increases.

The relative permittivity of the ALD-processed YDC thin layer is 10 times lower than that of the bulk material and, consequently, the structured thin film structured appears as a better dielectric material. The conductivity of the YDC thin layers becomes higher than that of YSZ thin layer at temperatures higher than 420 °C, which is within the range of the SOFC operating temperature. Thus, the use of this novel ALD-processed thin film structure appears to be a very important step forward in the design of SOFC devices with improved performance.

Acknowledgment. The authors acknowledge the financial support of the PICS Program 3746 between France and Finland.

(32) Da Yu Wang, D. S.; Park, J.; Griffith, A. S.; Nowick *Solid State Ionics* **1981**, *2*, 95–105.

(33) Sarkar, P.; Nicholson, P. S. *Solid State Ionics* **1986**, *21*, 49–53.